

Chapter 6 Laboratory Testing

6.1 Introduction

To study the relationships between soil electromagnetic properties and engineering properties, the engineering properties and electromagnetic properties of six natural soils and two pure clays were measured. These soils are the Staunton clay, Northern Virginia clay, Vicksburg Buckshot clay and Rome clay from Virginia, San Francisco Bay mud and Rancho Solano clay from California, Kaolin from Georgia and Na-bentonite from Wyoming. One-dimensional consolidation tests were performed on these soils using a batch consolidometer and five consolidation pressures from 4 psi to 50 psi. The compression index and coefficient of consolidation were determined from the deformation-time recordings. The hydraulic conductivity of these soils was calculated from the coefficient of consolidation and compressibility based on Terzaghi's 1D consolidation theory. At the end of each consolidation stage, the electromagnetic properties of these soils were measured using time domain reflectometry (TDR). The residual shear resistances of these soils under four normal stresses of 4 psi, 8 psi, 16 psi to 32 psi were measured using the ring shear apparatus. Specific surface area measurements were also made because the specific surface area is an important parameter linking the electromagnetic properties and engineering properties of fine-grained soils. After a review of the currently available techniques, the ethylene glycol monoethyl ether (EGME) adsorption method was chosen for the specific surface area measurement.

6.2 Soils and their physical properties

The Atterberg limits (liquid limit and plastic limit) of the eight soils were determined following the ASTM D4318 procedure. The soils were classified using the Unified Soil Classification System (USCS) plasticity chart as shown in Figure 6.1. The Atterberg limits and the USCS classification of these soils are listed in Table 6.1. All tests were performed on the portion of the soils passing the No. 40 sieve (425µm).

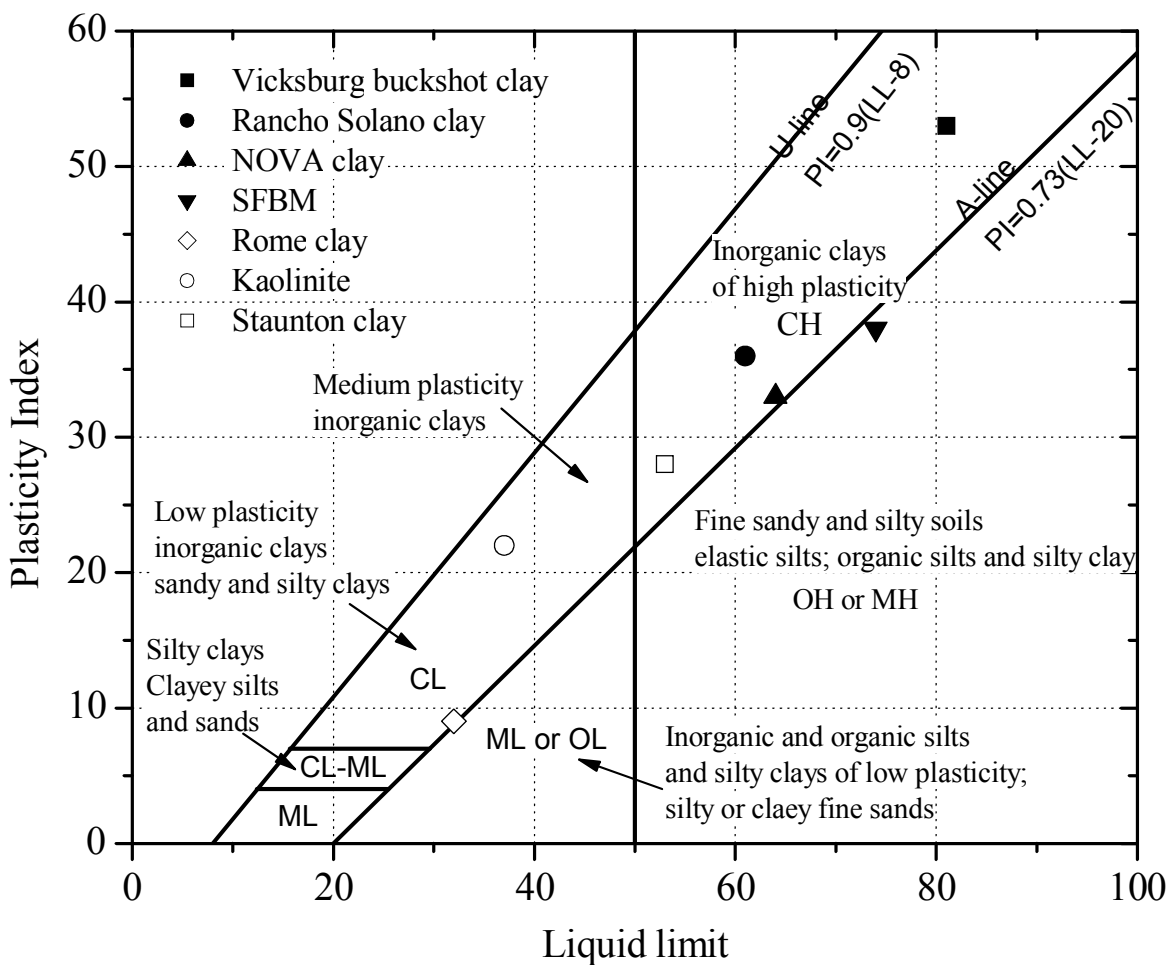


Figure 6.1 The Atterberg limits of the tested clay superimposed on the USCS plasticity chart

The mineralogical components of the Staunton clay, Northern Virginia clay, Vicksburg Buckshot clay and Rome clay were determined using X-ray diffraction (XRD) and thermal analysis (Geiman 2005). The tests were performed on the clay fraction (<2 µm) of these soils. The mineralogical compositions of the four clays are listed in Table 6.2.

Table 6.1 Engineering indexes of the eight soils being tested

Name	Source	USCS	Group Name	LL (%)	PL (%)	PI (%)	Specific Gravity
Staunton clay	Virginia	CH	Fat clay	53	25	28	2.74
Northern Virginia clay	Virginia	CH	Fat clay	64	31	33	2.8
Vicksburg Buckshot clay	Virginia	CH	Fat clay	81	28	53	2.79
Rome Clay	Virginia	CL	Lean clay	32	23	9	2.71
San Francisco Bay mud	California	MH	Gray elastic silt	74	36	38	2.7
Rancho Solano clay	California	CH	Brown fat clay	61	25	36	2.65
Kaolin	Georgia	CL	White lean clay	37	15	22	2.65
Na-Bentonite	Wyoming	CH	White Fat Clay	840	170	670	2.72

Table 6.2 Mineralogical compositions of the four natural soils being tested (on $-2 \mu\text{m}$ clay fraction)

Soil Name	Kao-linite	Mont-morillonite	Mica	Ver-miculite	HIV*	Gibbsite	Quartz	Feldspar	Amphi-bole
Staunton Clay	45%	20%	10%	10%	4%	1%	10%	-	-
Northern Virginia Clay	25%	35%	5%	15%	5%	3%	12%	-	-
Vicksburg Buckshot Clay	10%	60%	10%	15%	-	-	5%	-	-
Rome Clay	10%	5%	35%	20%	5%	-	15%	5%	5%
*HIV = Hydroxyle Interlayered Vermiculite									

6.3 Specific surface area measurement

Over the past several decades, many techniques have been developed to measure the specific surface area of fine-grained soils. These techniques can be generally divided into two categories - chemical adsorption and chemical absorption, as shown in Table 6.3.

Table 6.3 Summary of the currently available techniques to measure the specific surface area of clay

Category	Adsorbate types	Specific methods	References
Chemical adsorption	Gas molecules	Water vapor adsorption	(De Bruyn et al. 1957; Farrar and Coleman 1967; Sridharan et al. 1988)
		N ₂ -BET	(Churchman and Burke 1991; Hammel et al. 1983; Wetzel 1990)
	Organic liquids	Ethylene glycol	(Gill and Reaves 1957)
		Ethylene glycol monoethyl ether	(Cerato and Lutenegger 2002; Smith and Arulanandan 1981)
Chemical absorption	Methylene blue	MB spot	(Locat et al. 1984; Yukselen and Kaya 2006)
		MB titration	(Santamarina et al. 2002)

The most commonly used agent in chemical absorption method is methylene blue (MB) dye, which is positively charged in an aqueous solution. Thus, it will be absorbed to negatively charged clay surfaces when mixed with a soil suspension. Two procedures for MB absorption are the spot test (European standard) and the titration procedure. The spot test procedure involves adding the MB solution gradually to the soil suspension until no more MB dye can be absorbed by the clay surfaces. When this 'end' point is reached, a permanent light blue halo around the soil aggregates will be observed and the specific surface area of the soil can be determined from the amount of MB required to reach this end point. The precision of the MB absorption method can be improved by using a titration procedure. Details of the two procedures can be found in Yukselen and Kaya (2006).

Two types of adsorbate can be used in the chemical adsorption method: gas molecules and organic liquids. The mechanism of using gas molecules for soil specific surface area measurements is that the gas molecules close to the soil solid surface will be attracted by forces arising from the solid-phase surface atoms to form a monomolecular or multimolecular layer of gas molecules. From the amount of gas molecules being adsorbed at different pressure, the specific surface area of a soil can be calculated using the Brunauer, Emmette, and Teller (BET) equation (Brunauer et al. 1938). Two types of gas molecules are frequently used: water vapor and nitrogen. The water vapor adsorption method involves placing several grams of oven-dried soil samples into a vacuum desiccator and determining the amount of moisture being adsorbed to soil surfaces as a function of the relative water-vapor pressure. By assuming a single water molecule occupies a constant area on the soil surface, the area covered by the water molecules can

be determined. Details of water adsorption method can be found in Parfitt et al. (2001) and Ponizovskiy et al. (1993). The procedure for nitrogen adsorption is very similar to that for water vapor adsorption. However, the specific surface area determined from the nitrogen adsorption can be much lower than that from the water vapor adsorption method for high specific surface area minerals (de Jong 1999). This is partially because water molecules are small and they can penetrate into the micro-pores formed by clay aggregates and, partially because water molecules are polar and their adsorption to soil surfaces is relatively strong. In contrast, nitrogen molecules are large and non-polar. As a result, they can not penetrate into micro-pores formed by clay aggregates and their connection with soil surfaces is weak.

Organic liquids such as liquid glycerol, ethylene glycol (EG) or ethylene glycol monoethyl ether (EGME) can be used to measure the surface area of the predried and preweighted soil samples. The ethylene glycol (EG) method was developed by Dyal and Hendricks (1950). Following the same procedure of EG adsorption method, Carter et al. (1965) and Heilman et al. (1965) introduced a new polar solvent, EGME for adsorption. The EGME method has been adopted by USDA (USDA 1982) as a recommended procedure for total surface area measurement and it has gained popularity internationally because EGME equilibrates more rapidly with soils and clays than EG, yet gives the identical values (Tiller and Smith 1990). Therefore, the EGME adsorption method was adopted in this study to measure the specific surface areas of several clays.

6.3.1 Specific surface area measurements using the EGME method

A series of specific surface area measurements was performed in the Department of Crop and Soil Environmental Sciences at Virginia Tech. The measurements generally followed the procedure recommended by Cerato and Lutenegger (2002) with some modifications. The vacuum desiccator and dishes for specific surface area measurements are shown in Figure 6.2.



Figure 6.2 Dishes containing soil specimens placed in a desiccator for surface area measurement

The amount of EGME molecules was determined by weighing the soil samples before and after the adsorption of EGME molecules. The detailed procedure is listed in the Appendix. The adsorbed weight of EGME is converted to the specific surface area (m^2/g) using the following equation:

$$S_a = \frac{W_a}{0.000286W_s} \quad [6.1]$$

where W_a = weight of EGME retained by the sample (g); W_s = weight of oven-dried soil sample (g); 0.000286 = weight of EGME required for a mono-molecular EGME layer to cover a square meter of surface (g/m^2).

Four tests were performed for each soil. The measured specific surface areas from each test, the mean values and coefficient of variation are listed in Table 6.4. One specimen of the Rancho Solano clay was contaminated, and only three measurements are available for the Rancho Solano clay. The measured specific surface areas are also plotted in Figure 6.3 against the liquid limits of the soils.

When equation [6.1] is used to convert the adsorbed EGME to the specific surface area, two assumptions are implied: (1) A complete EGME monolayer is retained on both internal and external surfaces; (2) the factor converting the weight of the retained EGME to surface area is valid for all minerals and surfaces. Here, the conversion factor is chosen to be 0.000286 based on the recommendation of USDA (1982).

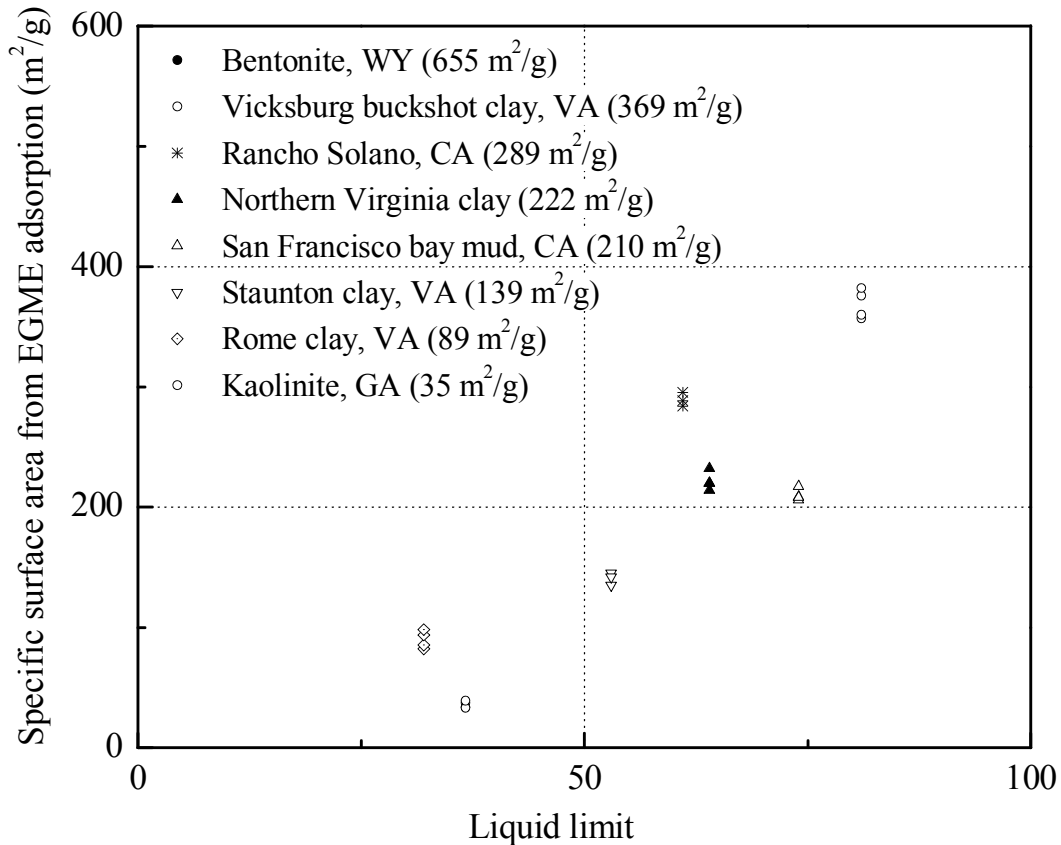


Figure 6.3 Specific surface areas of eight clays from the EGME adsorption method versus liquid limit

Table 6.4 Specific surface areas of eight clays from the EGME adsorption method

No. of Tests	Staunton clay	Northern Virginia clay	Vicksburg Buckshot clay	Rome clay	San Francisco bay mud	Rancho Solano clay	Kaolin	Na-bentonite
No.1 (m ² /g)	145.0	220.0	357.0	82.2	217.0	283.9	37.1	665.0
No.2 (m ² /g)	135.0	214.0	360.0	85.3	208.4	295.6	33.4	668.4
No.3 (m ² /g)	135.0	220.0	376.0	93.7	206.0	288.4	32.9	637.0
No.4 (m ² /g)	142.0	232.0	382.0	98.2	208.0	-	38.9	649.0
Average (m ² /g)	139.3	221.5	368.8	89.8	209.8	298.3	35.5	654.8
Coefficient of variation	3.2 %	3.0 %	2.9%	7.1%	2.0%	1.7%	7.1%	1.9%

6.4 Electromagnetic and engineering property measurements

All soil samples were mixed with distilled water and pushed through the #40 sieve (425 μm) to make slurries. The slurries with particle sizes less than #40 sieve size were prepared because both the specific surface area measurement using the EGME adsorption method and the residual shear strength measurements using the ring shear apparatus require that the maximum particle size of the soil sample be less than #40 sieve size.

The slurries were poured into a cylindrical batch consolidometer 5 inches in diameter and 4 inches in height. Two porous plates with a hydraulic conductivity much higher than that of the soil samples were placed beneath and upon the soil sample. Therefore, the samples were double-drained. Then, each of the soil samples was consolidated under pressures of 4 psi, 8 psi, 16 psi, 32 psi and 50 psi. The decrease of the sample height as a function of time under each consolidation pressure was recorded

6.4.1 Electromagnetic Properties

At the end of each consolidation, the cap of batch consolidometer and the top porous plate upon the soil specimen were removed. A three-rod TDR probe was slowly inserted into the soil, and the time-domain waveform of the soil was recorded. For each consolidation stage, six TDR measurements were performed. The batch consolidometer and the three-rod TDR probe are schematically shown in Figure 6.4.

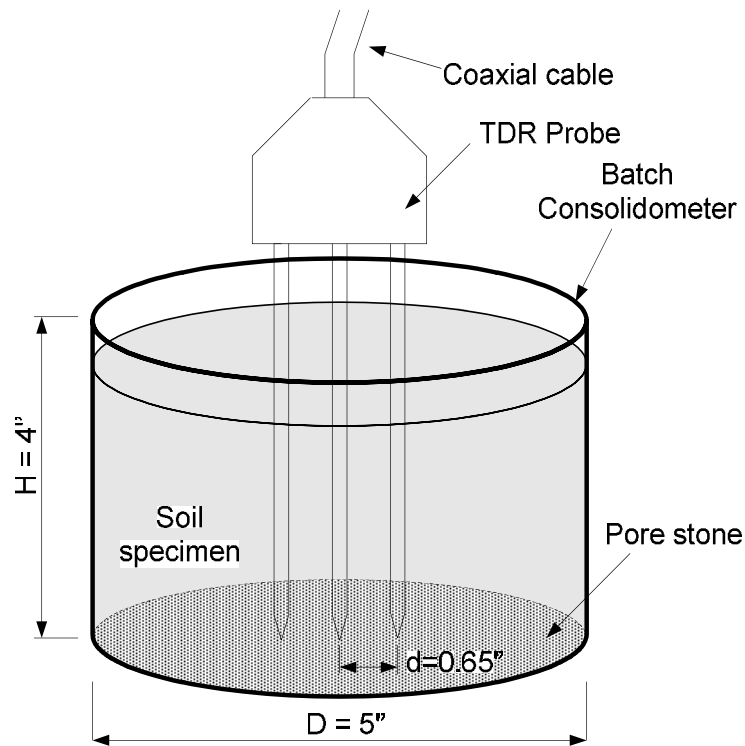


Figure 6.4 Illustration of a TDR probe inserted into the soil specimen in a batch consolidometer

The cylindrical rod of the TDR probe has a diameter of 3.15 mm. The distance between adjacent rods is approximately 16.5 mm (0.65 inches). The length of the rods is 150 mm, which is longer than the maximum thickness of the soil specimens. Thus, the rods were only partially inserted into the soil specimen and the thickness of the soil specimen at the time of measurement is equal to the penetration depth. The volume taken by the TDR rods is about 0.2 % of the sample volume in the batch consolidometer. Even though it is possible that the insertion of the probe caused some disturbances in the soil sample, the disturbance is considered to be small because the volume taken by the rods is very small.

The time-domain waveforms of the tested soils were recorded and plotted in Figures 6.5 to 6.11. The plotted time-domain waveforms at the end of each consolidation are the average of six measurements. The Vicksburg Buckshot clay is of high compressibility and the consolidation could not continue beyond the end of the third consolidation (16 Psi) because of the limitation of the batch consolidometer. Therefore, only three TDR waveforms were measured for the Vicksburg Buckshot clay. The San Francisco Bay mud was the first soil to be tested, for which the primary consolidation under each load had not been finished before a higher consolidation pressure was applied. Therefore, the differences between its waveforms are larger than other soils. Moreover, the compression index and coefficient of consolidation are not available for the San Francisco Bay mud.

The gravimetric water content of each soil at the end of the final consolidation was determined following the ASTM Standard (D2216). Then the volumetric water content at the end of the final consolidation can be calculated from the gravimetric water content w by:

$$\theta = \frac{w \cdot G_s}{1 + w \cdot G_s} \quad [6.2]$$

where G_s is the specific gravity of a soil, whose value is listed in Table 6.1 for the tested soils.

Since the specimens were consolidated from slurries, it can be assumed that they are fully saturated through the entire consolidation process. Therefore, the porosities at the end of other consolidation stages can be back-calculated from the final volumetric water content and the thickness of the specimen at the end of other consolidation stages:

$$n_i = 1 - \frac{H_f}{H_i} (1 - n_f) \quad [6.3]$$

where n_i and H_i are the porosity and sample height at the end of the i th consolidation; n_f and H_f are the porosity and sample height at the end of the final consolidation.

For fully saturated soils, the porosity n is equal to the volumetric water content θ . The void ratio is related to the porosity by:

$$e = \frac{n}{1-n} \quad [6.4]$$

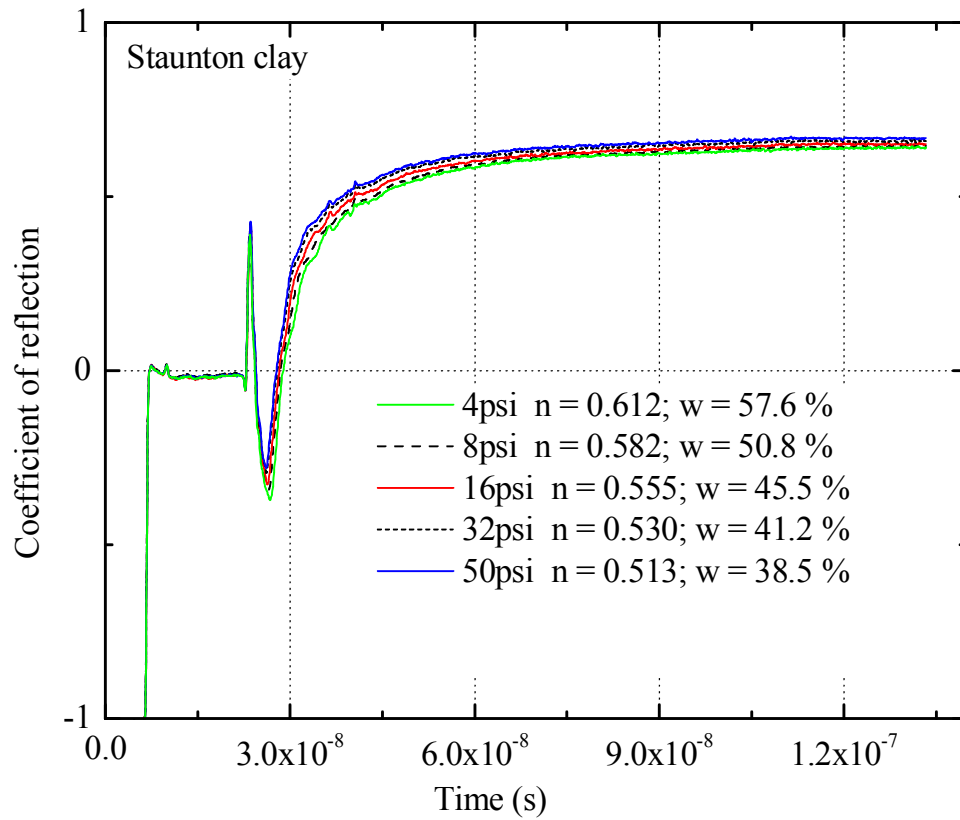


Figure 6.5 TDR waveforms of Staunton clay (n = porosity, w = gravimetric water content)

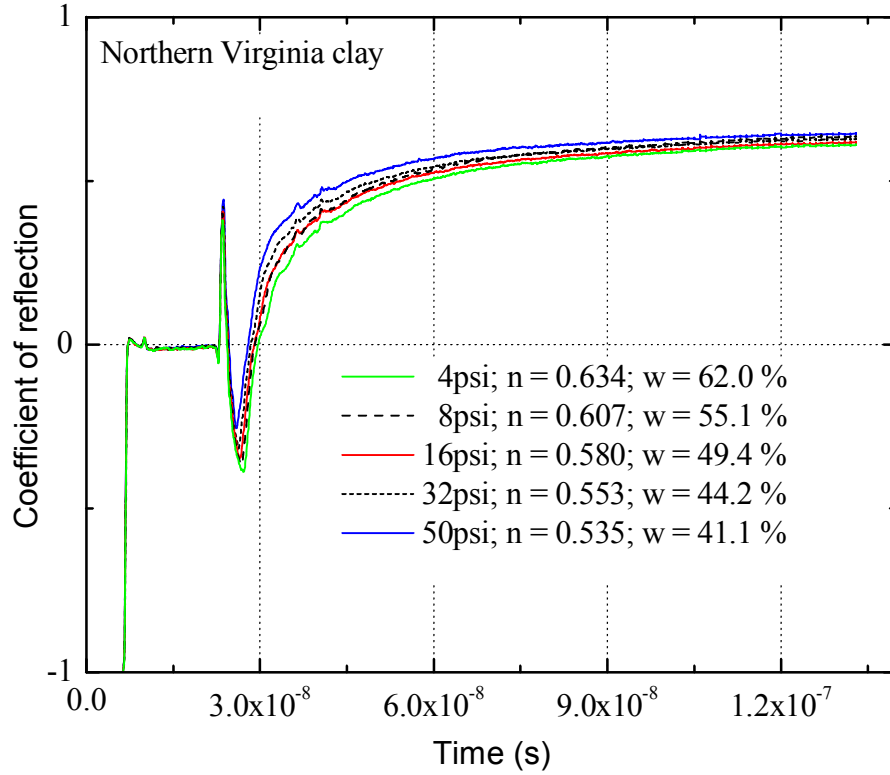


Figure 6.6 TDR waveforms of Northern Virginia clay (n = porosity, w = gravimetric water content)

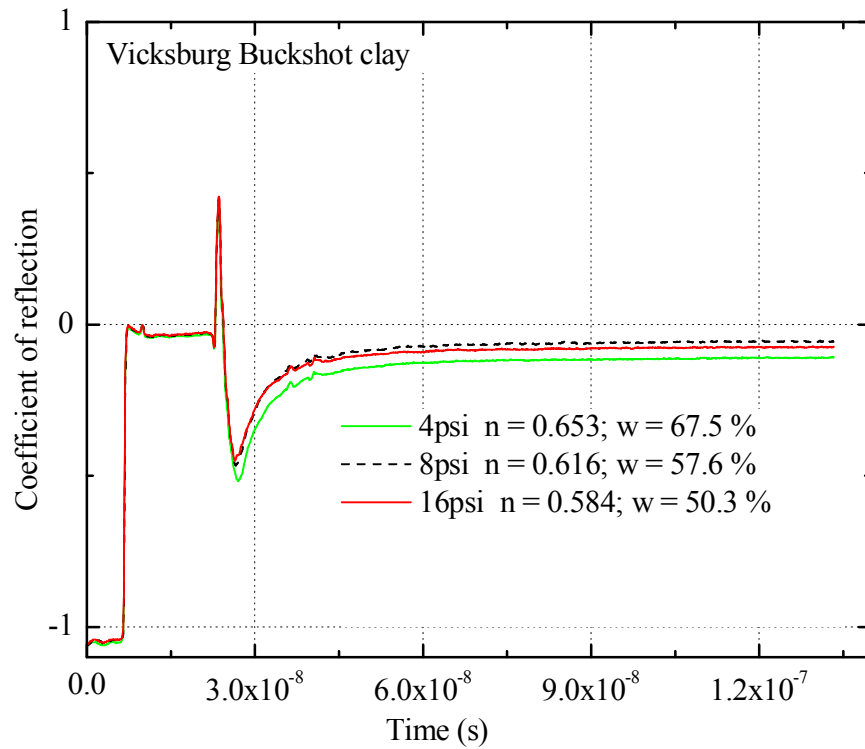


Figure 6.7 TDR waveforms of Vicksburg Buckshot clay

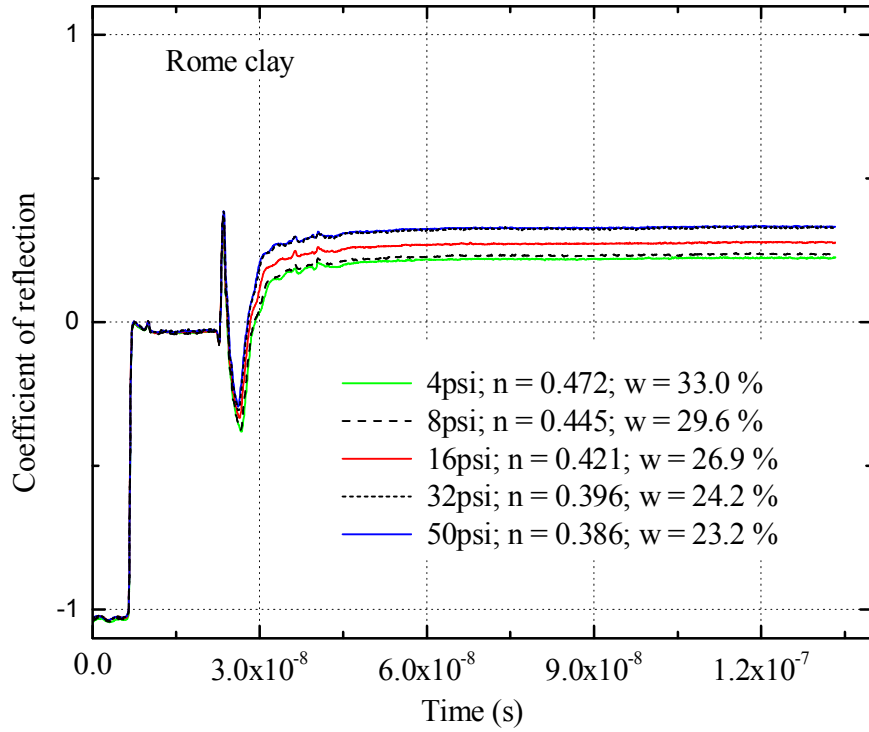


Figure 6.8 TDR waveforms of Rome clay (n = porosity, w = gravimetric water content)

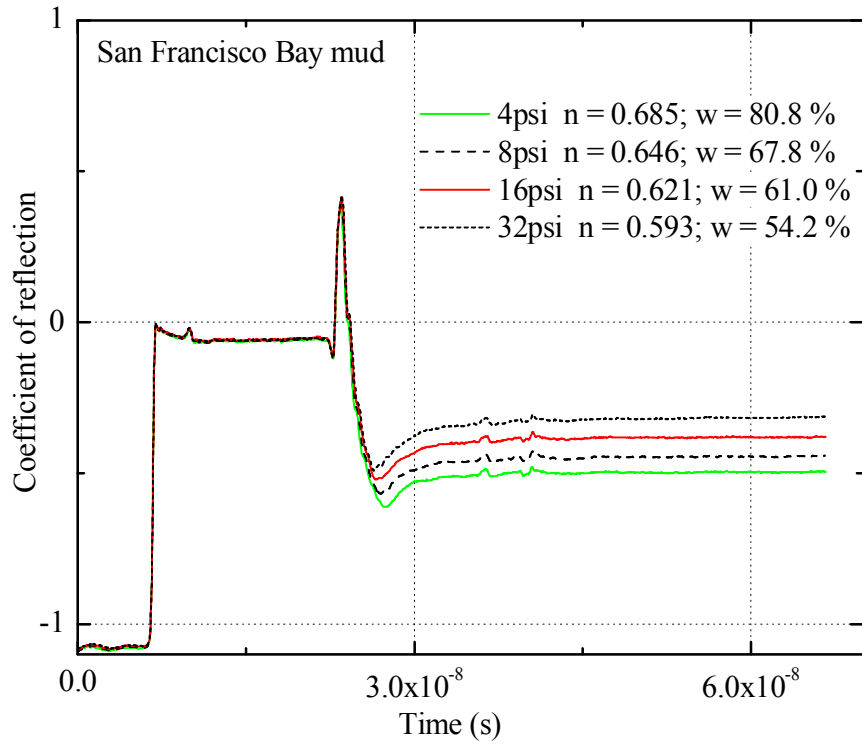


Figure 6.9 TDR waveforms of San Francisco Bay mud

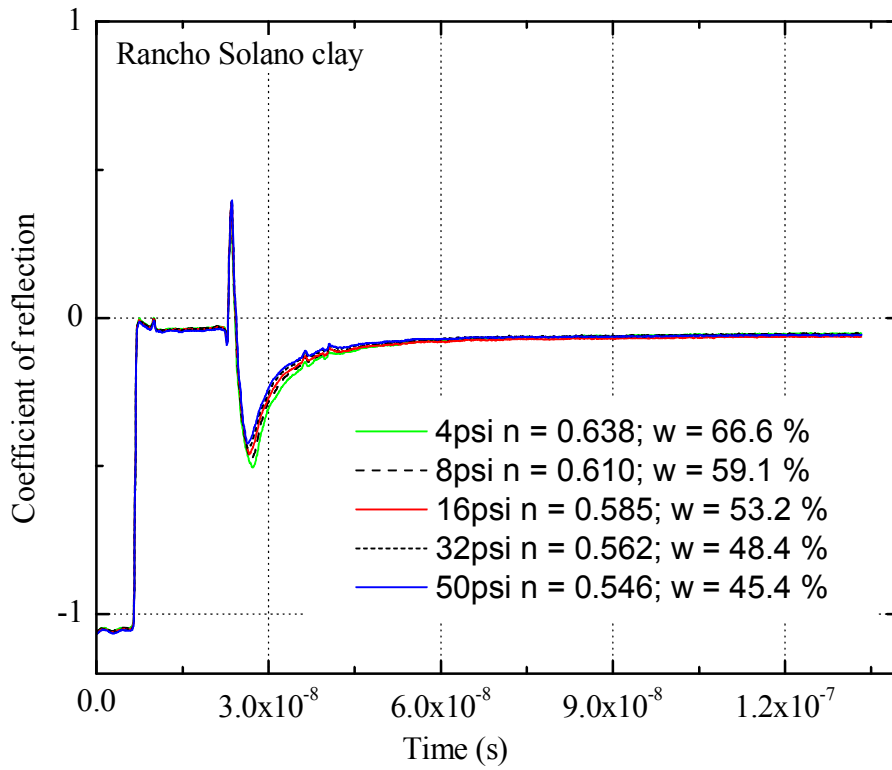


Figure 6.10 TDR waveforms of Rancho Solano clay (n = porosity, w = gravimetric water content)

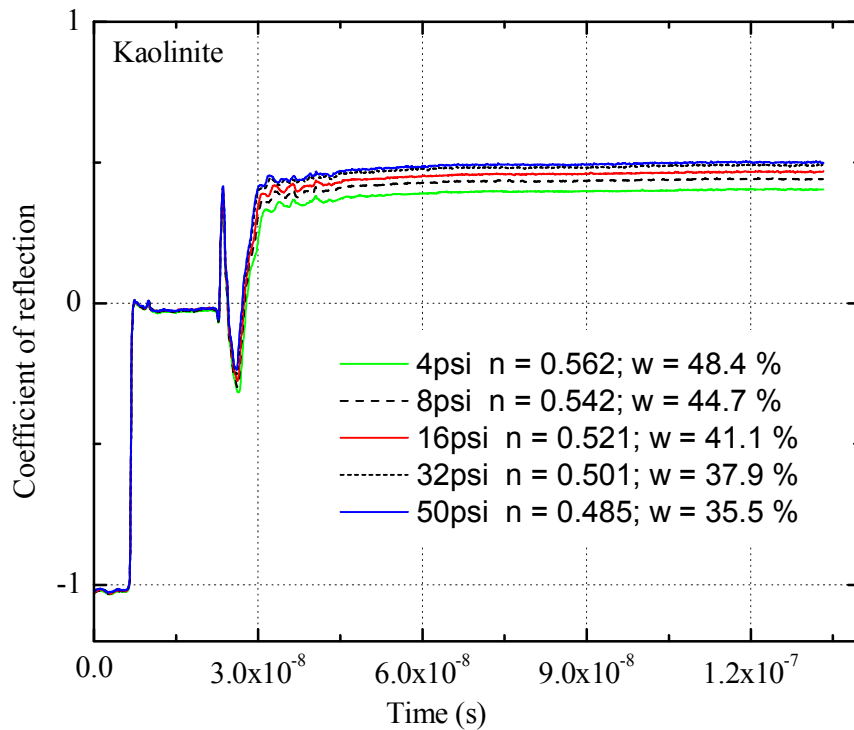


Figure 6.11 TDR waveforms of Kaolinite

6.4.2 Compressibility

The consolidation pressures shown in Figures 6.5 to 6.11 were read directly from a pressuremeter attached to the batch consolidometer. The actual pressures applied on the soil samples were slightly different from those read directly from the pressuremeter because the batch consolidometer deforms under high pressures. The batch consolidometer has been calibrated and a comparison between the directly read pressure and the actual pressure applied on soil samples is shown in Figure 6.12.

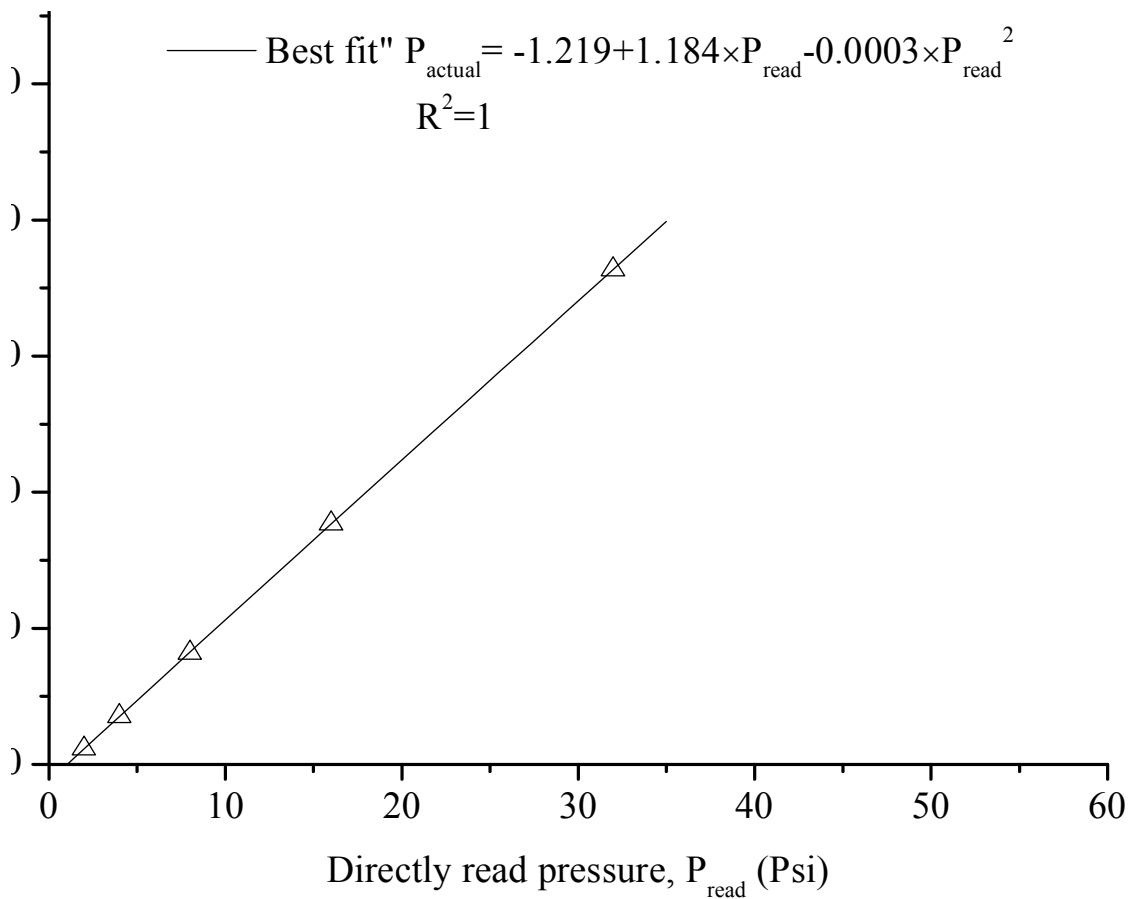


Figure 6.12 A comparison between the pressure applied on the soil sample and that read directly from the pressuremeter

The decrease of void ratio of the tested clays under each consolidation pressure is plotted in Figure 6.13 as a function of the consolidation pressure. Since the compression curves are not exactly straight, the compression index was calculated by fitting a straight line to the measured void ratio versus $\log \sigma'$ data points. The compression index C_c is defined as:

$$C_c = -de / d \log \sigma' \quad [6.5]$$

where e is the void ratio and σ' is the effective stress. The calculated compression indexes were normalized by the initial void ratio e_0 (void ratio at 4psi in this study) to obtain a compression ratio C_{ec} :

$$C_{ec} = C_c / (1 + e_i) \quad [6.6]$$

The compression indexes, initial void ratio and compression ratio are listed in Table 6.5.

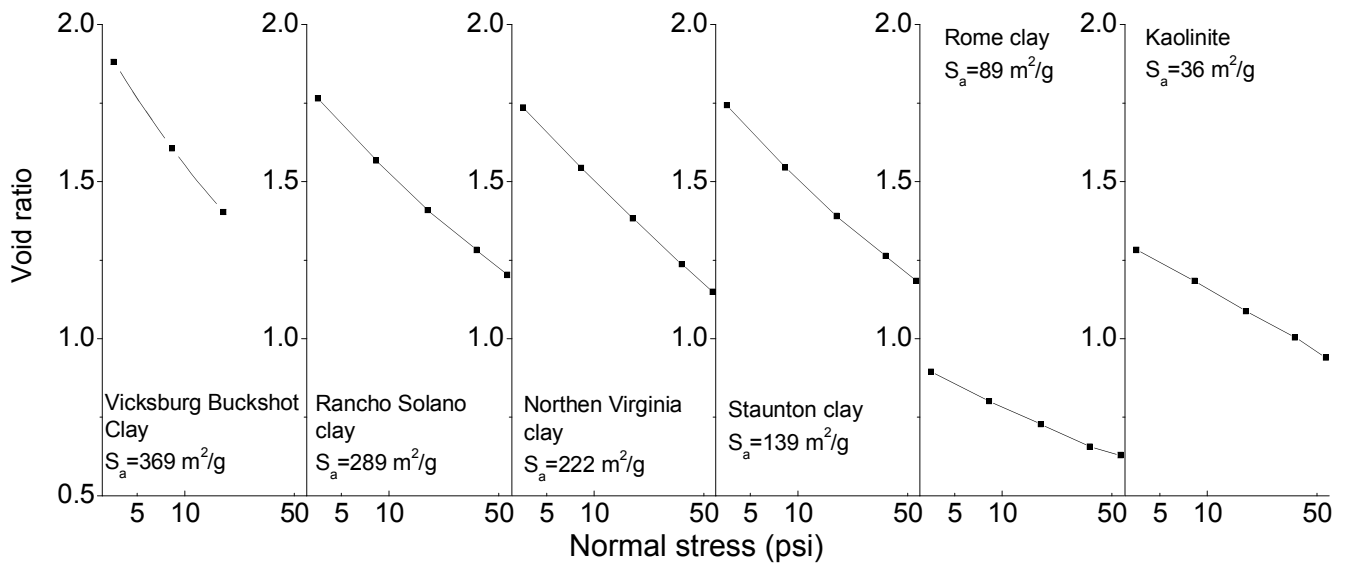


Figure 6.13 Compression curves of six clays

Table 6.5 Compression index, initial void ratio and compression ratio of six clays

	<i>Vicksburg Buckshot clay</i>	<i>Rancho Solano</i>	<i>Northern Virginia clay</i>	<i>Staunton clay</i>	<i>Rome clay</i>	<i>Kaolinite</i>
Compression index	0.300	0.200	0.210	0.187	0.096	0.122
Initial void ratio	1.882	1.766	1.736	1.579	0.895	1.283
Compression ratio	0.104	0.074	0.077	0.072	0.051	0.053

The compressibility m_v was also calculated for each soil being tested:

$$m_v = \frac{de}{(1+e_0)d\sigma'} \quad [6.7]$$

where de is the decrease of void ratio due to an increase in effective stress $d\sigma'$, e_0 is the void ratio before the increase of the effective stress. The coefficient of compressibility under each consolidation pressure is listed in Table 6.6 in together with the coefficient of consolidation.

6.4.3 Coefficient of consolidation

The compression of the soils versus time under each consolidation pressure was recorded. Typical consolidation curves are shown in Figure 6.14. Two methods, the Casagrande's method and Taylor's method, were used to determine the coefficient of consolidation c_v (m/s) from the time-compression data:

$$c_v = \frac{TH^2_{D50}}{t} \quad [6.8]$$

where T is a dimensionless time factor: the Casagrande's method uses 50% consolidation with $T=T_{50}=0.197$ and the Taylor's method uses 90% consolidation with $T=T_{90}=0.848$. t is the time corresponding to the particular degree of consolidation (s): the Casagrande's

method uses $t=t_{50}$ and the Taylor's method uses $t=t_{90}$. H_{D50} is the length of drainage path at 50% consolidation (m), corresponding to half the specimen height under each consolidation pressure. Details of the two methods can be found in the ASTM standard D2435-96 and Terzaghi, et al. (1996). The coefficients of consolidation from two methods under each consolidation pressure are plotted in Figure 6.15.

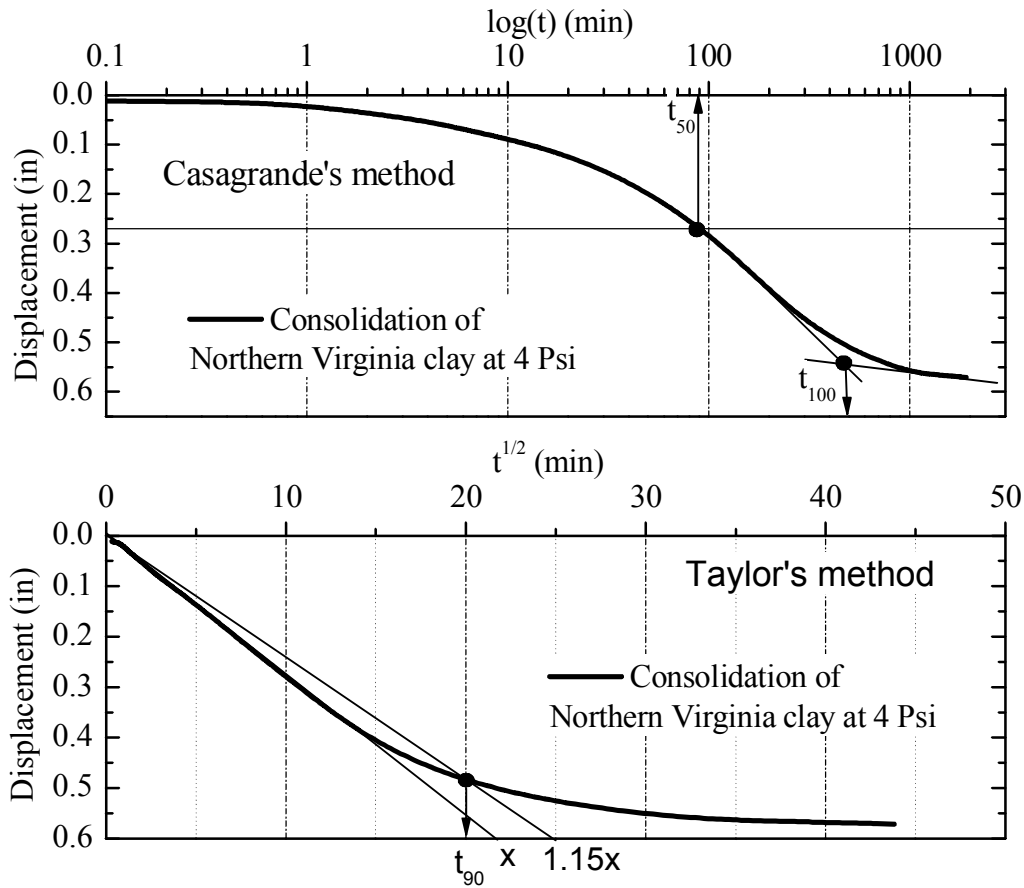


Figure 6.14 Consolidation of Northern Virginia clay at 4 Psi and the methods to determine the times corresponding to the 50 percent and 90 percent of consolidation

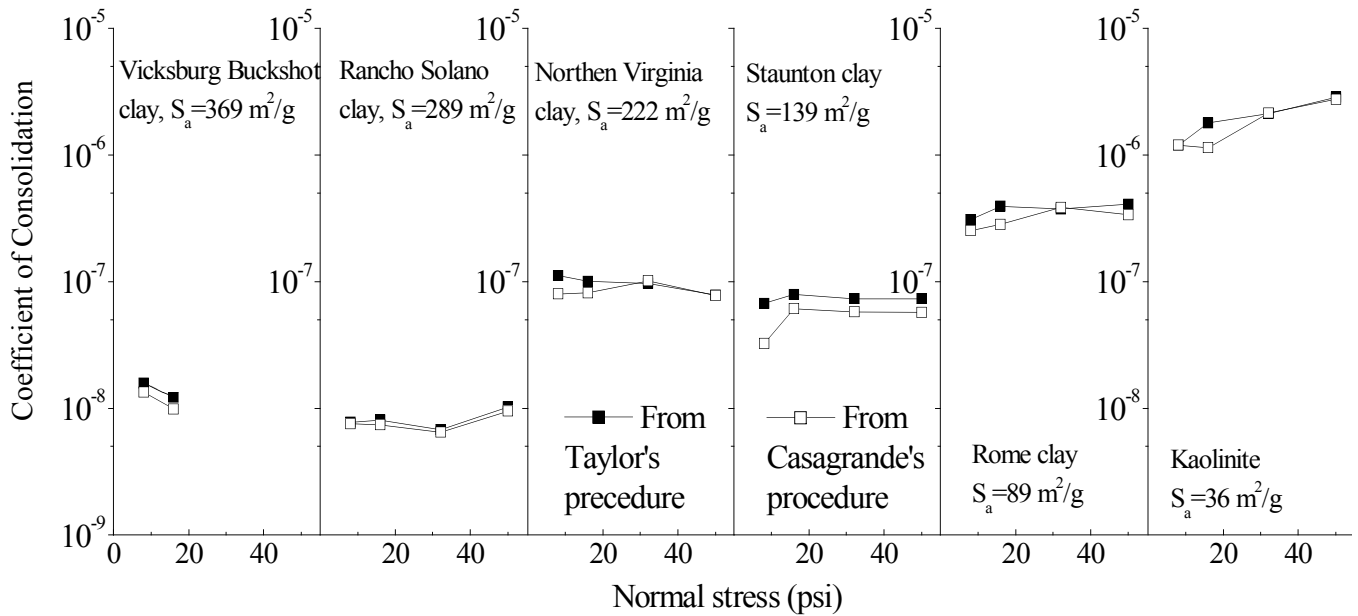


Figure 6.15 Coefficients of consolidation of six clays from two procedures

Generally, the coefficient of consolidation from the Taylor's method is higher than that from the Casagrande's method, which is also reflected by the measured data in the above figure.

According to Terzaghi's one dimensional consolidation theory, the hydraulic conductivity k_h in the vertical direction is related to the coefficient of consolidation c_v by:

$$k_h = m_v \cdot \frac{c_v \gamma_w}{d\sigma_v'} \quad [6.9]$$

where m_v is the compressibility (m^2/kN), γ_w is the unit weight of water (9.8 kN/m^3) and $d\sigma_v'$ is the increment in consolidation pressure (kN). Therefore, the hydraulic conductivities in the vertical direction can be calculated from the measured coefficient of consolidation and compressibility under each pressure increment as listed in Table 6.6.

Table 6.6 Coefficient of consolidation, compressibility, hydraulic conductivity and void ratio of six clays at the end of each consolidation pressure

Soil name	Consolidation pressure (psi)*	Void ratio at the end of each consolidation	Compressibility m_v (m ² /kN)	Coefficient of consolidation (m ² /s)		Hydraulic conductivity (m/s)	
				Casagrande's method (1)	Taylor's method (2)	Method (1)	Method (2)
Vicksburg Buckshot clay	3.5	1.882	-	-	-	-	-
	8.2	1.607	0.0035	1.35E-08	1.58E-08	4.57E-10	5.38E-10
	17.7	1.403	0.0014	9.89E-09	1.22E-08	1.37E-10	1.69E-10
Rancho Solano clay	3.5	1.766	-	-	-	-	-
	8.2	1.567	0.0026	7.59E-09	7.8E-09	1.94E-10	2E-10
	17.7	1.410	0.0011	7.45E-09	8.11E-09	8.08E-11	8.79E-11
	36.4	1.283	0.0005	6.52E-09	6.79E-09	3.06E-11	3.19E-11
	57.3	1.203	0.0003	9.51E-09	1.03E-08	2.63E-11	2.86E-11
Northern Virginia clay	3.5	1.736	-	-	-	-	-
	8.2	1.543	0.0026	8.04E-08	1.12E-07	2.02E-09	2.81E-09
	17.7	1.383	0.0011	8.16E-08	1.01E-07	9.11E-10	1.13E-09
	36.4	1.237	0.0006	1.02E-07	9.75E-08	5.54E-10	5.28E-10
	57.3	1.150	0.0003	7.79E-08	7.88E-08	2.4E-10	2.42E-10
Staunton clay	3.5	1.579	-	-	-	-	-
	8.2	1.393	0.0026	3.25E-08	6.72E-08	8.33E-10	1.72E-09
	17.7	1.247	0.0011	6.11E-08	7.91E-08	6.62E-10	8.58E-10
	36.4	1.128	0.0005	5.79E-08	7.32E-08	2.71E-10	3.43E-10
	57.3	1.054	0.0003	5.75E-08	7.36E-08	1.59E-10	2.03E-10
Rome clay	3.5	0.895	-	-	-	-	-
	8.2	0.801	0.0018	2.54E-07	3.11E-07	4.5E-09	5.5E-09
	17.7	0.728	0.0007	2.86E-07	3.95E-07	2.05E-09	2.83E-09
	36.4	0.656	0.0004	3.86E-07	3.77E-07	1.42E-09	1.39E-09
	57.3	0.629	0.0001	3.39E-07	4.1E-07	4.42E-10	5.34E-10
Kaolinite	3.5	1.283	-	-	-	-	-
	8.2	1.185	0.0016	1.2E-06	1.2E-06	1.83E-08	1.83E-08
	17.7	1.088	0.0008	1.15E-06	1.8E-06	9.01E-09	1.41E-08
	36.4	1.005	0.0004	2.16E-06	2.13E-06	7.62E-09	7.49E-09
	57.3	0.941	0.0003	2.77E-06	2.88E-06	6.98E-09	7.26E-09

* 1 psi = 6.895 kN/m²

6.4.4 Residual Shear Strength

The residual shear strength of soils were measured using the Bromhead ring shear device (Bromhead 1979) built by Wykeham Farrance Engineering Ltd. In order to minimize the overestimation of shear resistance of the soil caused by wall friction, the top platen of the conventional Bromhead ring shear device was modified by Meehan (2006) to reduce the entrapment of clay particles between the top platen and the side walls of the specimen container. The Bromhead ring shear device is widely used in engineering practice due to its capability of running shearing tests more quickly than other ring shear devices. The drained ring shear tests were performed following the procedures specified by ASTM Standard D 6467-99. Multistage tests were performed on each soil specimen by at first consolidating the soil specimen to the highest normal stress to be sheared, decreasing the normal stress to the lowest normal stress to be sheared, preshearing the specimen to one complete revolution, and then reshearing the specimen at several gradually increased normal stresses to its residual state. The shear resistance at the normal stresses of 4 psi, 8 psi, 16 psi and 32 psi were measured for each specimen to construct a residual shear stress τ versus normal stress σ_n plot as shown in Figure 6.16. For each soil, the relationship between τ and σ_n can be approximately fit by a straight line through the origin. The residual friction angle of a soil is determined from the inclination of the linear fit. The residual friction angle can also be determined using the secant phi approach (Stark and Eid 1994), which calculates the secant residual friction angle at each normal stress:

$$\phi_r = \text{Arc tan}(\tau / \sigma_n) \quad [6.10]$$

The residual friction angles from these two methods are listed in Table 6.7.

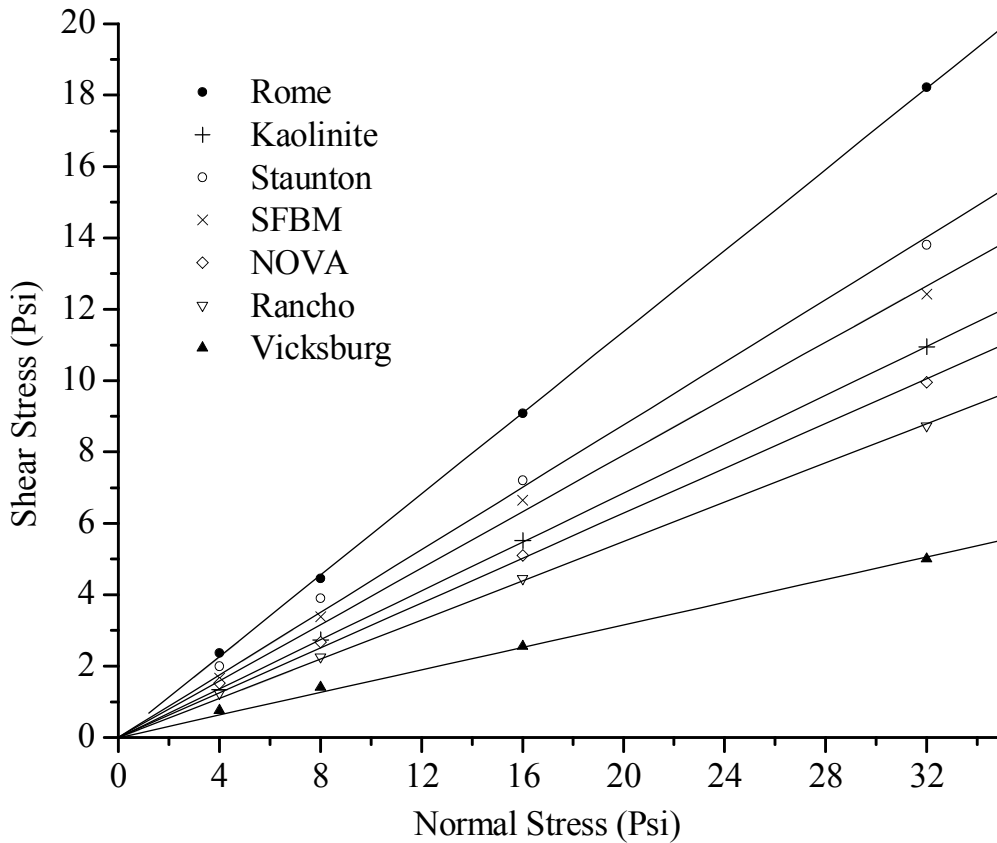


Figure 6.16 Shear stress versus normal stress from ring shear tests on seven clays

Table 6.7 Residual friction angles at different normal stresses

Pressure	Vicksburg Buckshot clay	Rancho Solano	Northern Virginia clay	San Francisco Bay mud	Staunton clay	Rome clay	Kaolinite
4 psi	10.6	17.2	20.8	22.5	26.6	30.6	18.6
8psi	9.9	15.7	18.5	23.0	26.0	29.1	18.9
16 psi	9.1	15.5	17.7	22.6	24.2	29.6	19.0
32 psi	8.9	15.3	17.3	21.2	23.3	29.7	18.9
Linear fit	9.0	15.4	17.5	21.6	23.7	29.6	18.9

Table 6.7 shows that the residual friction angle at low normal stresses is slightly higher than that at high normal stresses, which is consistent with the results from other studies (e.g., Meehan, 2006). The residual friction angle determined by fitting of the

experimental results with a straight line through origin is close to the residual friction angle determined for high normal stresses.

6.5 Summary

The electromagnetic properties and engineering properties of eight soils were measured in this study, including six natural soils and two pure clays. The soils were mixed with distilled water to make slurries and the slurries were consolidated under five consolidation pressures from 4 psi to 50 psi. At the end of each consolidation, the electromagnetic properties of these soils were measured using time domain reflectometry. The compression index and the coefficient of consolidation are determined from the time-deformation records of these soils. The hydraulic conductivities of these soils in the vertical direction are calculated from the coefficient of consolidation using the Terzaghi's 1D consolidation theory. The residual shear strengths of these soils are measured by the ring shear test.

Several commonly used methods to measure the specific surface area of clay are introduced. The ethylene glycol monoethyl ether (EGME) adsorption method was chosen to measure the specific surface areas of the clays tested in study. The detailed procedure of the EGME adsorption method is described.

The method of transforming the TDR time-domain waveforms to the frequency domain dielectric spectrum will be described in the next chapter. The relationship between the electromagnetic properties, total specific surface area and engineering properties will be discussed in Chapter 8.